J Fluoresc (2010) 20:67–72
DOI 10.1007/s10895-009-0523-6

ORIGINAL PAPER

Relative Quantum Yield Measurements of Coumarin Encapsulated in Core-Shell Silica Nanoparticles

Erik Herz · Thomas Marchincin · Laura Connelly · Daniel Bonner · Andrew Burns · Steven Switalski · Ulrich Wiesner

Received: 4 May 2009 / Accepted: 21 July 2009 / Published online: 18 August 2009

Abstract Fluorescent silica nanoparticles encapsulating organic fluorophores provide an attractive materials platform for a wide array of applications where high fluorescent brightness is required. We describe a class of fluorescent silica nanoparticles with a core-shell architecture and narrow particle size distribution, having a diameter of less than 20 nm and covalently incorporating a blue-emitting coumarin dye. A quantitative comparison of the scattering-corrected relative quantum yield of the particles to free dye in water yields an enhancement of approximately an order of magnitude. This enhancement of quantum efficiency is consistent with previous work on rhodamine dye-based particles. It provides support for the argument that improved brightness over free dye in aqueous solution is a more general effect of covalent incorporation of fluorescent organic dyes within rigid silica nanoparticle matrices. These results indicate a synthetic route towards highly fluorescent silica nanoparticles that produces excellent probes for imaging, security, and sensing applications.

Keywords Fluorescent nanoprobe · Nanoparticle · Fluorescence · Relative quantum yield · Silica

E. Herz · L. Connelly · D. Bonner · A. Burns · U. Wiesner (✉)
Department of Materials Science and Engineering,
Cornell University,
Ithaca, NY 14853, USA
e-mail: ubw1@cornell.edu

T. Marchincin · S. Switalski
Research Laboratories, Eastman Kodak Company,
Rochester, NY 14650, USA

Present address:
L. Connelly
University of California, San Diego,
La Jolla, CA 92093, USA

Present address:
D. Bonner
Department of Chemical Engineering,
Massachusetts Institute of Technology,
Cambridge, MA 02139, USA

Present address:
A. Burns
GE Global Research,
Niskayuna, NY 12309, USA

Introduction

Since the discovery of fluorescence in quinine sulfate solution over 160 years ago, the use and study of fluorescence as a tool for imaging, sensing, and security applications has led to a wide array of probes used to track, tag, sense, and separate [1]. All of these applications benefit from brighter, more stable, and environmentally robust fluorescent probes and much research has been devoted to this challenge. The most commonly used probes are fluorescent dyes, quantum dots, and fluorescent particles, each with their own advantages and disadvantages [2].

Organic fluorescent dyes come in a multitude of absorption and emission wavelengths, are extremely small (making them compatible on the scale of e.g. molecular biology), and many have been refined and specialized to operate in specific environments with the highest possible brightness. Unfortunately, many potential applications subject these dyes to harsh environments, including acidic or basic extremes, enzymatic activity, and interactions with ions [3, 4]. These environments may quench the dye's emission through chemical interactions with its structure or cause aggregation or self-quenching that is due to insolubility of the dye [3]. Colloidal semiconductor quantum dots

are a relatively new class of very bright, quantum-confined inorganic materials that have garnered significant attention as nanoscale fluorescent probes. They have several advantages over dyes, including narrow emission, broad short-wavelength excitation, and highly tunable size dependent emission wavelengths [5]. However, their production, use, and disposal present a challenge to the scientific and industrial communities because of their heavy metal content [6, 7]. Finally, hybrid fluorescent particles, which incorporate fluorophores within a polymeric or inorganic matrix, are another class of probes that endeavor to combine the best properties of the dyes with those of the matrix [4, 8–10]. Through incorporation into a matrix material, a fluorescent dye can be protected from the surrounding environment which is in turn protected from any toxicity, to create benign probes [11, 12]. The homogeneous entrapment of dyes within a matrix has been accomplished in several ways, but may lead to particles with some dyes that are not well protected and can interact with or leach into the surrounding environment [13].

The Wiesner group has recently developed a class of core-shell silica nanoparticles, referred to as C dots [2, 14–18]. The particle synthesis approach, using a modified Stöber technique, provides a materials platform with a number of advantages over existing fluorescent probes including: (i) defined placement of covalently bound fluorescent dyes that do not leach, (ii) small particle sizes and size distributions, (iii) control over particle architecture and color, and (iv) enhanced brightness and photostability as compared to the parent dye in water [2, 14–18]. Here we describe the synthesis of coumarin dye containing C dots and investigate the per-dye enhanced fluorescent properties, over free dye in aqueous solution, by means of relative quantum yield analysis. One effect that has not been accounted for in previous C dot work is the contribution of scattering. To this end, for the present study we chose a blue absorbing and emitting coumarin dye, for which scattering effects should be at a maximum, and covalently encapsulated it within a core-shell silica particle. Quantum efficiency enhancements were assessed using scattering-corrected relative quantum yield measurements.

Relative quantum yield is a reproducible measure of a fluorescent probe's efficiency in converting absorbed photons to emitted photons relative to a reference standard of known quantum yield and was chosen for this study for its spectral flexibility [19]. The standard acts to calibrate the instrumentation and methods used to measure the absorption and integrated emission of all samples, input that is then used to calculate the relative quantum yield. The relative quantum yield also provides a means to compare fluorescent probes of different composition and type to each other using one of the most important measures of performance, the efficiency of emission.

Experimental section

Fluorescent core-shell silica nanoparticles were produced for this work by a three-step synthesis illustrated in Fig. 1a–c, based on modifications to the Stöber method for producing pure silica particles [20]. First, a 2 mL solution of 7-diethylaminocoumarin-3-carboxylic acid, succinimidyl ester (DEAC, 4.5 mM in dimethylformamide, Anaspec) was conjugated to 3-aminopropyltriethoxysilane (APTS, 0.45 mmol, Gelest) while stirring in a nitrogen atmosphere glove box for 12 h. The resulting conjugate was removed from the glove box, added to a 500 mL stirring mixture of ethanol, water, and ammonia (2.0 M in ethanol, Sigma-Aldrich) in a 7.43 : 0.4275 : 0.1 mole ratio and allowed to equilibrate. Immediately thereafter, 0.025 mol tetraethylorthosilicate (TEOS, Sigma-Aldrich, Inc.) was added and allowed to co-condense with the conjugated dye for 12 h to produce a dye-rich core. Finally, pure TEOS was added stepwise to synthesize the pure silica shell of desired thickness that protects the core and dyes within it. The TEOS was added slowly in order to avoid secondary nucleation [21]. After synthesis, particles were stored in darkness in the reaction solution until needed, and in this way are both chemically and colloidally stable for at least 6 months.

In order to properly compare the relative quantum yield of a dye encapsulated in the C dots versus free dye, a scattering correction was performed. To this end, same-sized blank core-shell silica particles containing no dye were produced by removing the dye and the conjugation step from the

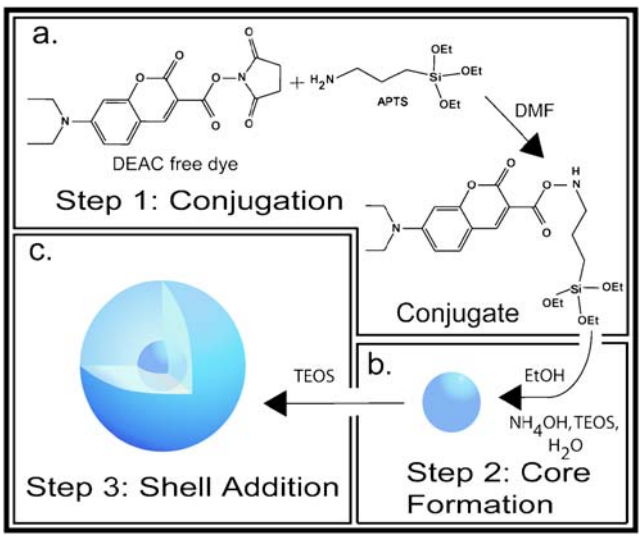

Fig. 1 Core-shell fluorescent silica nanoparticle synthesis: **a** Conjugation of 7-diethylaminocoumarin-3-carboxylic acid, succinimidyl ester (DEAC) dye with 3-aminopropyltriethoxysilane (APTS) to form the dye-silicate precursor; **b** Core formation using tetraethoxysilane (TEOS) and the conjugate in basic ethanol and water solution; **c** Addition of pure TEOS to form a protective shell

synthesis procedure described above and adding the APTS directly to the particle core synthesis (Fig. 1b).

Because of their small size, purification of all particles was accomplished by dialysis into 18.2 MΩ/cm deionized water (deionized by a Millipore Synthesis system), using 3500 MWCO dialysis tubing (Snakeskin, Pierce). Particles were dialyzed (1:500) for 8–12 h and subsequently filtered through a 0.2 μm pore size syringe filter. After purification, the physical attributes of the freshly dialyzed particles were characterized using dynamic light scattering and scanning electron microscopy (SEM, LEO 1550 FE-SEM). Dynamic light scattering (DLS, Malvern Zetasizer Nano ZS) provides the hydrodynamic particle size and particle size distribution while SEM allows for the real space observation of size and shape. SEM was performed on a polished silicon wafer substrate upon which the particles were deposited from a dilute ethanol solution of water-dialyzed particles to speed drying of the deposited sample.

After investigating the physical particle attributes, fluorescence and absorption measurements on the particles, constituent dye, and a standard dye were performed in preparation for relative quantum yield calculations. The spectrophotometer (Varian Cary 5E) was calibrated by checking the baseline, performing a spectral position check (using a holmium oxide standard SRM 2034), and finally by checking the photometric response (using an SRM 930D NIST transmittance standard glass filter, nominal 20% transmittance, 0.7045 absorbance at 546 nm). The spectrofluorometer (Jobin Yvon Spex Fluorolog Tau 3) was calibrated using the Raman peak of water at 397 nm when excited at 350 nm. All calibrations for the equipment used were performed daily and logs thereof retained. For the spectrophotometer, a solution of blank particles was used as a reference standard to correct for the aforementioned difference in scattering between free dye and particles in aqueous solution. The correction was achieved by matching the scattering intensity of the blank and dye-containing particles at short wavelengths and subsequent spectral subtraction. For the spectrofluorometer, all emission spectra were corrected using a standard lamp with a NIST traceable calibration.

After calibrating the instruments, samples of DEAC-based fluorescent nanoparticles and the free dye were diluted with water to an absorption-matched molar concentration of between 10^{-6} and 10^{-7} moles/L of dye molecules (whether free in solution or encapsulated within the particles). The NIST reference material (SRM 936), quinine sulfate dihydrate, dissolved in 1N H_2SO_4, was selected for its spectral overlap with DEAC and its good quantum yield of 0.546 [22]. The standard was freshly prepared. Each sample was placed in a 10 cm path length optical glass cell for spectrophotometry measurements. An aliquot of the spectrophotometry sample was then taken for fluorometry measurements in a 1 cm path length quartz cell. Both measurements were performed thrice on each sample to ensure repeatability and minimize effects of local temperature fluctuations on absorption measurements.

For the calculation of relative quantum yield, from scattering corrected spectra, the following equation was used [19]:

$$\phi_s = \phi_{st} \frac{A_{st}}{A_s} \frac{F_s}{F_{st}} \left(\frac{n_s}{n_{st}} \right)^2 \quad (1)$$

The ratio of the quinine sulfate reference standard absorption (A_{st}) to the absorption of the sample (A_s), at 380 nm, was found first and multiplied by the quantum yield [22] of the quinine sulfate solution (ϕ_{st}) as well as the squared ratio of the sample refractive index (n_s) corrected to be that of water, 1.33, and the reference standard refractive index (n_{st}), 1.34 [23]. This product was then multiplied by

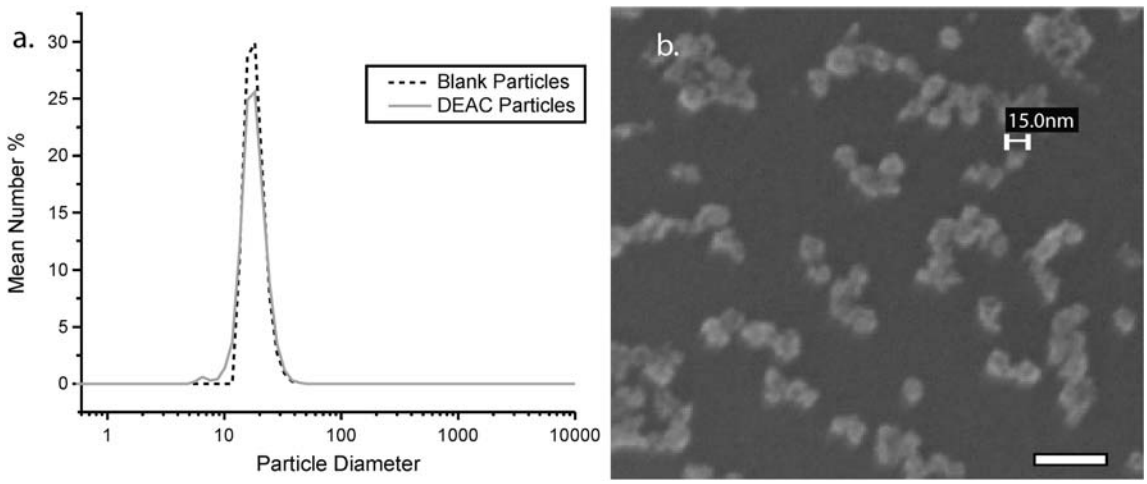

Fig. 2 **a** Results of dynamic light scattering measurements of blank silica and DEAC-containing silica particles used in this study. **b** Representative scanning electron microscopy image of DEAC-containing core-shell particles (scale bar=50 nm), corroborating DLS results

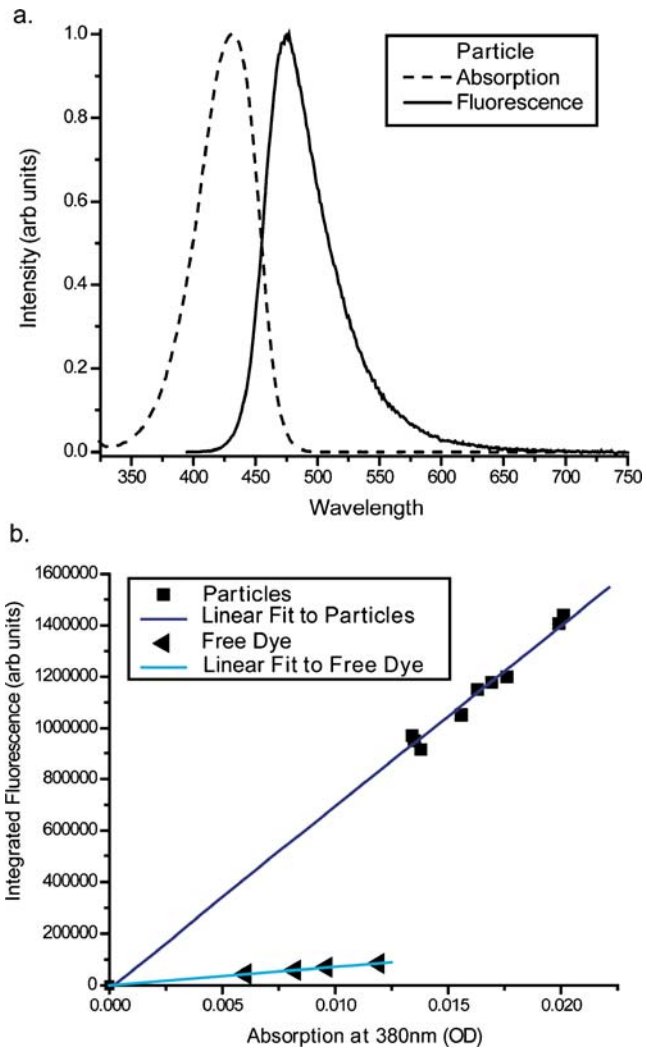

Fig. 3 **a** Normalized and scattering corrected absorption and normalized fluorescence for DEAC containing core-shell silica nanoparticles in water; **b** Integrated fluorescence as a function of absorption at 380 nm for particles and free dye

the ratio of the integrated area under the emission spectrum (from 395 to 750 nm) of the sample (F_s) to that of the standard (F_{st}) to find the relative quantum yield of the particles and free dye. Note that the excitation wavelength of 380 nm was used as it provides the spectral position of maximum overlap of the absorption spectra of the quinine sulfate reference and DEAC dyes.

Results and discussion

The synthesis reaction conditions reproducibly yielded sub 20 nm particles. Dynamic light scattering results indicate that the DEAC-based particles and the blank silica particles are both approximately 18 nm in diameter based on number statistics (see Fig. 2a). A representative SEM image of the DEAC-based particles is shown in Fig. 2b, corroborating the DLS results on size and demonstrating the narrow particle size distribution. From spectrophotometry and spectrofluorometry the absorption and fluorescence spectra of the particles were collected in water. Representative plots of normalized and corrected fluorescence and absorption spectra are shown in Fig. 3a for the particles in water. Figure 3b depicts fluorescence as a function of absorption at 380 nm for a series of dye and particle samples. From this plot it is evident that the particles are significantly brighter than the free dye. The linear fits of the data include the zero fluorescence at zero absorption point. The quality of the fits implies that no reabsorption of fluorescence is occurring.

From the data in Fig. 3b and use of Eq. 1, the relative quantum yield, ϕ_s, for the particles is 0.178 (±0.0178) while that for the dye is only 0.02 (±0.002) [24]. The results demonstrate an approximately ten-fold increase in quantum yield achieved by covalently encapsulating the dye within a core-shell silica nanoparticle. To the best of our knowledge this is the largest enhancement reported to date for a fluorophore encapsulated in a sub 20 nm silica nanoparticle. In order to rule out conjugation effects on the enhancement, a sample of DEAC was conjugated to 4-amino-1-butanol through the succinimidyl ester reactive moiety on the dye and compared to free dye by absorption matching aqueous solutions at 380 nm and then comparing the emission. The results are shown in Figure 4 and indicate that, if anything, the free dye is brighter than the conjugated one. Hence, the silica matrix of the nanoparticles clearly allows for more efficient light emission from encapsulated DEAC dye molecules relative to free dye in solution, a finding consistent with our previous work on other dye families [16, 17]. For a rhodamine-based C dot we found

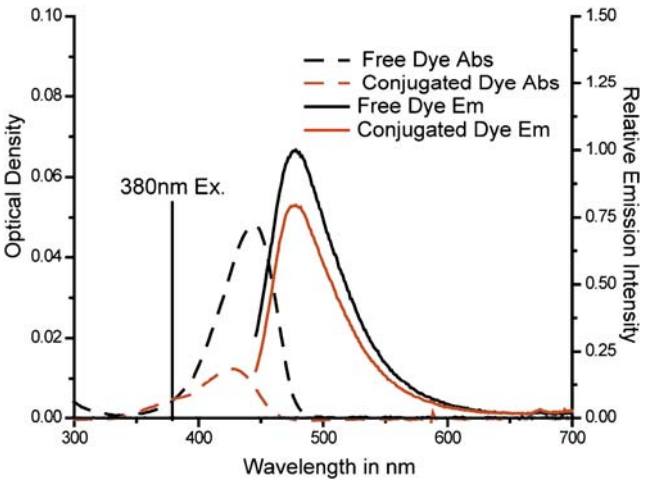

Fig. 4 DEAC free dye compared to DEAC dye conjugated to 4-amino-1-butanol to test effect of conjugation only (i.e. without encapsulation in silica). The resulting conjugate, absorption matched at 380 nm is slightly less bright than the free dye, indicating that the enhancement observed in the particles is not due to conjugation, but rather the encapsulation

that the covalent encapsulation of multiple dye molecules lead to 30 nm particles close to 30 times brighter than the single dye molecule in water [17]. This brightness enhancement over free dye could be accounted for by the product of the per-dye quantum efficiency enhancement and the number of dyes per particle. Small changes in the internal architecture of the C dots were found to enhance the quantum efficiency up to three-fold on a per-dye basis, with no observable energy transfer between dyes for up to about 10 dyes per 5 nm core in a 30 nm diameter particle. The quantum efficiency increase was due to a uniform two-fold enhancement in the radiative rate and a reduction in the nonradiative rate, which was found to vary inversely with the degree of rotational mobility the dye experienced within the silica particle matrix. These results taken together with the current work provide strong support for the argument that silica, with a glass transition temperature about an order of magnitude above that of organic polymers, is an especially well-suited matrix for dye-encapsulation because it provides a particularly rigid local environment that enhances dye performance.

Conclusions

In summary, we have reported on the synthesis of fluorescent core-shell silica nanoparticles with diameters between 15 and 20 nm, incorporating a blue-emitting dye, 7-diethylaminocoumarin-3-carboxylic acid succinimidyl ester. The dye's relative quantum yield, as measured by means of scattering-corrected relative quantum yield analysis, is enhanced by an order of magnitude over that of the free dye in water. The results demonstrate that the C dot architecture can lead to significant improvements of the photophysical properties of organic fluorophores in water by sequestering them away from the solvent into a rigid, solid-state silica-type environment that itself is compatible with water. The enhanced relative quantum yield, combined with the ability to incorporate multiple dyes per particle, leads to significantly increased probe brightness as compared to free dye, making these particles excellent candidates for imaging, security, and sensing applications. These results, taken together, demonstrate a practical method for synthesizing highly fluorescent silica nanoparticles. Enhancing the performance of dyes through encapsulation in core-shell silica nanoparticles may significantly reduce costs and at the same time catapult performance characteristics of relatively inexpensive dyes to levels competitive with optimized fluorescent probes.

Acknowledgments The authors thank the Army for funding through award number W911NF-06-C-0124, in collaboration with the NEI Corporation. Special thanks to the Cornell Center for Materials Research for facility use as well as the Keck FE-SEM facility and facility manager Mick Thomas for his advice on imaging the particles. Support for the CCMR is provided through the NSF Grant DMR 0520404, part of the NSF MRSEC Program.

References

1. Herschel SJFW (1845) On a case of superficial colour presented by a homogeneous liquid internally colourless. Phil Trans Roy Soc London 135:143–145
2. Burns A, Ow H, Wiesner U (2006) Fluorescent core–shell silica nanoparticles: towards Lab on a Particle architectures for nanobiotechnology. Chem Soc Rev 35:1028–1042
3. Lakowicz JR (1999) Principles of fluorescence spectroscopy, 2nd edn. Kluwer Academic/Plenum, New York
4. Rampazzo E, Bonacchi S, Montalti M, Prodi L, Zaccheroni N (2007) Self-organizing core-shell nanostructures: spontaneous accumulation of dye in the core of doped silica nanoparticles. J Am Chem Soc 129:14251–14256
5. Murray CB, Norris DJ, Bawendi MG (1993) Synthesis and characterization of nearly monodisperse CdE (E=sulfur, selenium, tellurium) semiconductor nanocrystallites. J Am Chem Soc 115:8706–8715
6. Chang E, Thekkek N, Yu WW, Colvin VL, Drezek R (2006) Evaluation of quantum dot cytotoxicity based on intracellular uptake. Small 2:1412–1417
7. Derfus AM, Chan WCW, Bhatia SN (2004) Probing the cytotoxicity of semiconductor quantum dots. Nano Lett 4:11–18
8. Wang F, Tan WB, Zhang Y, Fan W, Wang M (2006) Luminescent nanomaterials for biological labelling. Nanotechnology 17:R1–R13
9. Bosma G, Pathmamanoharan C, de Hoog EHA, Kegel WK, van Blaaderen A, Lekkerkerker HNW (2002) Preparation of monodisperse, fluorescent PMMA-latex colloids by dispersion polymerization. J Colloid Interf Sci 245:292–300
10. Pagliaro M, Ciriminna R, Man MWC, Campestrini S (2006) Better chemistry through ceramics: the physical bases of the outstanding chemistry of ORMOSIL. J Phys Chem B 110:1976–1988
11. Choi J, Burns A, Williams RM, Zhou Z, Flesken-Nikitin A, Zipfel W, Wiesner U, Nikitin AY (2007) Core-shell silica nanoparticles as fluorescent biological labels for nanomedicine applications. J Biomed Opt 12(6):1–11
12. Graf C, Schartl W, Fischer K, Hugenberg N, Schmidt M (1999) Dye-labeled poly(organosiloxane) microgels with core-shell architecture. Langmuir 15:6170–6180
13. Zhao X, Bagwe RP, Tan W (2004) Development of organic-dye-doped silica nanoparticles in a reverse microemulsion. Adv Mater 16:173–176
14. Burns A, Sengupta P, Zedayko T, Baird B, Wiesner U (2006) Core/shell fluorescent silica nanoparticles for chemical sensing: towards single-particle laboratories. Small 2:723–726
15. Fuller JE, Zugates GT, Ferreira LS, Ow H, Nguyen NN, Wiesner U, Langer RS (2008) Intracellular delivery of core-shell fluorescent silica nanoparticles. Biomaterials 29(10):1526–1532
16. E. Herz, A. Burns, S. Lee, P. Sengupta, D. Bonner, H. Ow, C. Liddell, B. Baird and U. Wiesner, (2006), Fluorescent core-shell silica nanoparticles: an alternative radiative materials platform, Proceedings of SPIE Vol. 6096. doi:10.1117/12.661782
17. Larson DR, Ow H, Vishwasrao HD, Heikal AA, Wiesner U, Webb WW (2008) Silica nanoparticle architecture determines

radiative properties of encapsulated fluorophores. Chem Mater 20 (8):2677–2684
18. Ow H, Larson DR, Srivastava M, Baird BA, Webb WW, Wiesner U (2005) Bright and stable core-shell fluorescent silica nanoparticles. Nano Lett. 5(1):113–117
19. Williams ATR, Winfield SA (1983) Relative fluorescence quantum yields using a computer-controlled luminescence spectrometer. Analyst 108:1067–1071
20. Stöber W, Fink A, Bohn E (1968) Controlled growth of monodisperse silica spheres in the micron size range. J Colloid Interf Sci 26:62–69
21. Nyffenegger R, Quellet C, Ricka J (1993) Synthesis of fluorescent, monodisperse, colloidal silica particles. J Colloid Interf Sci 159:150–157
22. Melhuish WH (1961) Quantum efficiencies of fluorescence of organic substances: effect of solvent and concentration of the fluorescent solute. J Phys Chem 65:229–235
23. Sulfuric Acid vs. Refractive Index (20°C), (Mettler Toledo, 2008) p. http://us.mt.com/mt/ed/appEdStyle/Sulfuric_Acid_re_e_0x000248e10002599200076416.jsp
24. Stated error in quantum yield of quinine sulfate dihydrate NIST reference material (SRM 936) given at 10%